arXiv:1107.2775v2 [hep-ph] 7 Nov 2011

DESY 10-059
UWThPh-2011-22

Flavour violating gluino three-body decays at LHC

A. Bartl[1], H. Eberl[2], E. Ginina[1], B. Herrmann[3], K. Hidaka[4], W. Majerotto[2] and W. Porod[5]

[1] *Universität Wien, Fakultät für Physik, A-1090 Vienna, Austria*
[2] *Institut für Hochenergiephysik der Österreichischen Akademie der Wissenschaften, A-1050 Vienna, Austria*
[3] *Deutsches Elektronen-Synchrotron (DESY), Theory Group, D-22603 Hamburg, Germany*
[4] *Department of Physics, Tokyo Gakugei University, Koganei, Tokyo 184-8501, Japan*
[5] *Institut für Theoretische Physik und Astrophysik, Universität Würzburg, D-97074 Würzburg, Germany*

Abstract

We study the effect of squark generation mixing on gluino production and decays at LHC in the Minimal Supersymmetric Standard Model (MSSM) for the case that the gluino is lighter than all squarks and dominantly decays into three particles, $\tilde{g} \to q\bar{q}\tilde{\chi}_k^0$, $q\bar{q}'\tilde{\chi}_l^\pm$. We assume mixing between the second and the third squark generations in the up-type and down-type squark sectors. We show that this mixing can lead to very large branching ratios of the quark-flavour violating gluino three-body decays despite the strong constraints on quark-flavour violation (QFV) from the experimental data on B mesons. We also show that the QFV gluino decay branching ratios are very sensitive not only to the generation mixing in the squark sector, but also to the parameters of the neutralino and chargino sectors. We show that the branching ratio of the QFV gluino decay $\tilde{g} \to c\bar{t}(\bar{c}t)\tilde{\chi}_1^0$ can go up to $\sim 40\%$. Analogously, that of the QFV decay $\tilde{g} \to s\bar{b}(\bar{s}b)\tilde{\chi}_1^0$ can reach $\sim 35\%$. We find that the rates of the resulting QFV signatures, such as $pp \to tt\bar{c}\bar{c}E_{\rm T}^{mis}$, can be significant at LHC. This could have an important influence on the gluino searches at LHC.

1 Introduction

The flavour structure of the quark sector is very well described by the Cabibbo-Kobayashi-Maskawa (CKM) mixing matrix, which is the only source of quark flavour violation (QFV) in the Standard Model (SM). In particular, flavour changing neutral current (FCNC) processes, such as $K^0 \to \mu^+\mu^-$, $B^0 \to \mu^+\mu^-$, $B \to X_s\gamma$, $B \to X_s\, l^+l^-$ etc., are strongly suppressed [1]. They impose strong constraints on the quark generation mixing. Any extension of the SM must therefore respect these constraints.

In supersymmetric (SUSY) extensions of the SM, mixing between different quark flavours in the squark sector, that is not related to the CKM-matrix is also possible. Although the mixing between the first and second generation squarks is strongly constrained, there is room for appreciable mixing between the second and third generation of squarks, still obeying the constraints from B meson data[1]. This is beyond the minimal flavour violation (MFV), where the only source of QFV is the mixing due to the CKM matrix [3, 4, 5].

The effects of mixing between the second and third squark generations, especially the mixing between top and charm squarks, have been studied in the Minimal Supersymmetric Standard Model (MSSM) for squark production and decays at LHC [6, 7, 8, 9, 10]. Squark generation mixing has been investigated in detail in the QFV decays of gluinos, $\tilde{g} \to \bar{\tilde{u}}_{1,2}\, c\, (\tilde{u}_{1,2}\, \bar{c}) \to c\, \bar{t}\, \tilde{\chi}_1^0\, (\bar{c}\, t\, \tilde{\chi}_1^0)$, where $\tilde{u}_{1,2}$ are the lightest squark states and are mixtures of charm and top squarks [11]. There it is assumed that at least one squark is lighter than the gluino, so that the gluino decays first into a real squark (antisquark) and an antiquark (quark). In [11] it is shown that this leads to pronounced edge structures in the charm top-quark invariant mass distribution.

In the present paper we study the QFV gluino decays in the general MSSM assuming that all squarks are heavier than the gluino, so that the gluino dominantly decays into three particles. This will give rise to a very different pattern of QFV gluino decays as compared to the studies in Ref. [11], due to interference effects between the various virtual squark exchange contributions. Moreover, the invariant mass distributions will have different shapes without any edge structure in contrast to the case studied in [11].

We study the mixing between the second and the third generations not only in the up-type squark sector as in Ref. [11], but also in the down-type sector. We investigate QFV gluino decays including those into down-type quark pair plus neutralino, such as $\tilde{g} \to s\bar{b}\tilde{\chi}_1^0$. Furthermore, we also investigate in detail the dependence of the QFV gluino decay branching ratios on the neutralino/chargino parameters. We take into account all relevant experimental constraints on the MSSM parameters from B physics and searches for Higgs bosons and SUSY particles, and the theoretical constraints on the trilinear couplings from the vacuum stability conditions.

Recently ATLAS and CMS performed searches for SUSY at LHC with $\sqrt{s} = 7$ TeV on the basis of total integrated luminosities of 35 pb^{-1} [12, 13] and ~ 1 fb^{-1} [14, 15]. They found no excess of events over the SM expectations and set limits on the squark and

[1]There could also be mixing between the right up-squark and the left top-squark which is hardly constrained [2]. However, we do not consider this mixing here.

gluino masses at 95% confidence level (CL). In the simplified SUSY model with $m_{\tilde{\chi}_1^0} \approx 0$ (where all SUSY particles other than the gluino and squarks of the first two generations, and $\tilde{\chi}_1^0$ are decoupled by being given very heavy masses) the limit on the gluino mass is $m_{\tilde{g}} \gtrsim 800$ GeV for large $m_{\tilde{q}}$ and that on the squark mass is $m_{\tilde{q}} \gtrsim 850$ GeV for large $m_{\tilde{g}}$ [14] (see [15] also). Here, $m_{\tilde{q}}$ is the degenerate mass of the squarks of the first two generations. In the context of the constrained MSSM (CMSSM) (or mSUGRA) the lower limit on the gluino mass is smaller than ∼650 GeV for $m_{\tilde{q}} \gtrsim 1.5$ TeV and the limit on the squark mass is $m_{\tilde{q}} \gtrsim 1.1$ TeV for any $m_{\tilde{g}}$ [15, 16] (see [14] also). Here again $m_{\tilde{q}}$ is defined to be the degenerate mass of the squarks of the first two generations and the masses of the third generation squarks are (significantly) smaller than this $m_{\tilde{q}}$ in this framework of the CMSSM (mSUGRA). Therefore we will assume a gluino mass of about 1 TeV in our analysis respecting these gluino mass limits.

2 Squark mixing with flavour violation

In the MSSM the most general form of the squark mass matrices in the super-CKM basis of $\tilde{q}_{0\gamma} = (\tilde{q}_{1\mathrm{L}}, \tilde{q}_{2\mathrm{L}}, \tilde{q}_{3\mathrm{L}}, \tilde{q}_{1\mathrm{R}}, \tilde{q}_{2\mathrm{R}}, \tilde{q}_{3\mathrm{R}})$, $\gamma = 1, ...6$, where $(q_1, q_2, q_3) = (u, c, t), (d, s, b)$ is [17]

$$\mathcal{M}^2_{\tilde{q}} = \begin{pmatrix} \mathcal{M}^2_{\tilde{q},LL} & \mathcal{M}^2_{\tilde{q},LR} \\ \mathcal{M}^2_{\tilde{q},RL} & \mathcal{M}^2_{\tilde{q},RR} \end{pmatrix}, \tag{1}$$

for $\tilde{q} = \tilde{u}, \tilde{d}$, where the 3×3 matrices read

$$\begin{aligned} \mathcal{M}^2_{\tilde{d},LL} &= M_Q^2 + D_{\tilde{d},LL}\mathbf{1} + \hat{m}_d^2, & \mathcal{M}^2_{\tilde{u},LL} &= V_{\mathrm{CKM}} M_Q^2 V_{\mathrm{CKM}}^\dagger + D_{\tilde{u},LL}\mathbf{1} + \hat{m}_u^2, \\ \mathcal{M}^2_{\tilde{d},RR} &= M_D^2 + D_{\tilde{d},RR}\mathbf{1} + \hat{m}_d^2, & \mathcal{M}^2_{\tilde{u},RR} &= M_U^2 + D_{\tilde{u},RR}\mathbf{1} + \hat{m}_u^2. \end{aligned} \tag{2}$$

Here $M^2_{Q,U,D}$ are the hermitian soft-SUSY-breaking mass matrices of the squarks and $\hat{m}_{u,d}$ are the diagonal mass matrices of up- and down-type quarks. $D_{\tilde{q},LL} = \cos 2\beta m_Z^2 (T_3^q - e_q \sin^2\theta_W)$ and $D_{\tilde{q},RR} = e_q \sin^2\theta_W \cos 2\beta m_Z^2$, where T_3^q and e_q are the isospin and electric charge of the quarks (squarks), respectively, and θ_W is the weak mixing angle. The left-left blocks of the up-type and down-type squark mass matrices are related by the CKM matrix V_{CKM} due to the $\mathrm{SU(2)_L}$ symmetry. Note that $V_{\mathrm{CKM}} M_Q^2 V_{\mathrm{CKM}}^\dagger \simeq M_Q^2$ as $V_{\mathrm{CKM}} \simeq 1$. The off-diagonal blocks of eq. (1) read

$$\begin{aligned} \mathcal{M}^2_{\tilde{d},RL} = \mathcal{M}^{2\dagger}_{\tilde{d},LR} &= \frac{v_1}{\sqrt{2}} T_D^T - \mu^* \hat{m}_d \tan\beta, \\ \mathcal{M}^2_{\tilde{u},RL} = \mathcal{M}^{2\dagger}_{\tilde{u},LR} &= \frac{v_2}{\sqrt{2}} T_U^T - \mu^* \hat{m}_u \cot\beta\,. \end{aligned} \tag{3}$$

Here $T^T_{U,D}$ are transposes of $T_{U,D}$ which are the soft-SUSY-breaking trilinear coupling matrices of the up-, down-type squarks: $\mathcal{L}_{int} \supset -(T_{U\alpha\beta}\tilde{u}^\dagger_{R\beta}\tilde{u}_{L\alpha}H_2^0 + T_{D\alpha\beta}\tilde{d}^\dagger_{R\beta}\tilde{d}_{L\alpha}H_1^0)$, μ is the higgsino mass parameter, and $\tan\beta = v_2/v_1$, where $v_{1,2} = \sqrt{2}\left\langle H^0_{1,2}\right\rangle$ are the vacuum

Table 1: Constraints on the MSSM parameters from the B-physics experiments relevant mainly for the mixing between the second and the third generations of squarks, and from the Higgs sector. The fourth column shows constraints at 95% CL obtained by combining the experimental error quadratically with the theoretical uncertainty, except for $B(B_s \to \mu^+\mu^-)$ and m_{h^0}, which is the mass of the lighter CP-even neutral Higgs boson. $R^{\rm SUSY}_{B\to\tau\nu}\equiv\frac{{\rm B(B^+\to\tau^+\nu)_{SUSY}}}{{\rm B(B^+\to\tau^+\nu)_{SM}}} \approx [1-((m_{B^+}\tan\beta)/m_{H^+})^2]^2$, where m_{H^+} is the charged Higgs boson mass [19].

Observable	Exp. data	Theor. uncertainty	Constr. (95%CL)
ΔM_{B_s} [ps^{-1}]	17.77 ± 0.12 (68% CL) [1]	± 3.3 (95% CL) [20]	17.77 ± 3.31
$10^4\times$B$(b \to s\gamma)$	3.55 ± 0.26 (68% CL) [21]	± 0.23 (68% CL) [22]	3.55 ± 0.68
$10^6\times$B$(b \to s\ l^+l^-)$			
$(l = e$ or $\mu)$	1.60 ± 0.50 (68% CL) [23]	± 0.11 (68% CL) [24]	1.60 ± 1.00
$10^8\times$B$(B_s \to \mu^+\mu^-)$	< 4.3 (95% CL) [25]		< 4.3
$10^4\times$B$(B^+ \to \tau^+\nu)$	1.68 ± 0.31 (68% CL) [21]	± 0.25 (68% CL) [21]	$R^{\rm SUSY}_{B\to\tau\nu} = 1.40 \pm 0.76$
m_{h^0} [GeV]	> 114.4 (95% CL) [1, 26]	± 4.0 [27]	> 110.4

expectation values of the neutral Higgs fields. The squark mass matrices are diagonalized by the 6×6 unitary matrices $R^{\tilde{q}}$, $\tilde{q} = \tilde{u}, \tilde{d}$, such that

$$R^{\tilde{q}}\mathcal{M}^2_{\tilde{q}}(R^{\tilde{q}})^\dagger = {\rm diag}(m^2_{\tilde{q}_1}, \ldots, m^2_{\tilde{q}_6}) \qquad \text{with} \qquad m_{\tilde{q}_1} < \ldots < m_{\tilde{q}_6}\ . \tag{4}$$

The physical mass eigenstates $\tilde{q}_i, i = 1, ..., 6$ are given by $\tilde{q}_i = R^{\tilde{q}}_{i\alpha}\tilde{q}_{0\alpha}$.

In accordance with [18] we define the QFV parameters $\delta^{LL}_{\alpha\beta}$, $\delta^{uRR}_{\alpha\beta}$ and $\delta^{uRL}_{\alpha\beta}$ $(\alpha \neq \beta)$ as follows:

$$\delta^{LL}_{\alpha\beta} \equiv M^2_{Q\alpha\beta}/\sqrt{M^2_{Q\alpha\alpha}M^2_{Q\beta\beta}}\ , \tag{5}$$

$$\delta^{uRR}_{\alpha\beta} \equiv M^2_{U\alpha\beta}/\sqrt{M^2_{U\alpha\alpha}M^2_{U\beta\beta}}\ , \tag{6}$$

$$\delta^{uRL}_{\alpha\beta} \equiv (v_2/\sqrt{2})T_{U\beta\alpha}/\sqrt{M^2_{U\alpha\alpha}M^2_{Q\beta\beta}}\ . \tag{7}$$

Here $\alpha, \beta = 1, 2, 3$ $(\alpha \neq \beta)$ denote the quark flavours. The QFV parameters in the up-type squark sector relevant for this study are δ^{LL}_{23}, δ^{uRR}_{23}, $\delta^{uRL}_{23} = (\delta^{uLR}_{32})^*$ and $\delta^{uLR}_{23} = (\delta^{uRL}_{32})^*$ which are the $\tilde{c}_L - \tilde{t}_L$, $\tilde{c}_R - \tilde{t}_R$, $\tilde{c}_R - \tilde{t}_L$ and $\tilde{c}_L - \tilde{t}_R$ mixing parameters, respectively. For the down-type squark sector we define the QFV parameters as follows $(\alpha \neq \beta)$:

$$\delta^{dRR}_{\alpha\beta} \equiv M^2_{D\alpha\beta}/\sqrt{M^2_{D\alpha\alpha}M^2_{D\beta\beta}}\ , \tag{8}$$

$$\delta^{dRL}_{\alpha\beta} \equiv (v_1/\sqrt{2})T_{D\beta\alpha}/\sqrt{M^2_{D\alpha\alpha}M^2_{Q\beta\beta}}\ . \tag{9}$$

The QFV parameters in the down-type squark sector relevant for our study are δ^{LL}_{23}, δ^{dRR}_{23}, $\delta^{dRL}_{23} = (\delta^{dLR}_{32})^*$ and $\delta^{dLR}_{23} = (\delta^{dRL}_{32})^*$ which are the $\tilde{s}_L - \tilde{b}_L$, $\tilde{s}_R - \tilde{b}_R$, $\tilde{s}_R - \tilde{b}_L$ and $\tilde{s}_L - \tilde{b}_R$ mixing parameters, respectively.

In our analysis we neglect mixing between the first two squark generations due to the severe experimental constraints from K meson physics. We also neglect mixing between the first and third squark generations focusing on the effects of mixing between the second and third generations. We assume all the QFV parameters to be real. These parameters are also subject to the experimental constraints given in Table 1.

Furthermore we impose the vacuum stability conditions for the trilinear coupling matrices [28]

$$|T_{U\alpha\alpha}|^2 \;<\; 3\; Y_{U\alpha}^2\; (M_{Q\alpha\alpha}^2 + M_{U\alpha\alpha}^2 + m_2^2)\;, \tag{10}$$

$$|T_{D\alpha\alpha}|^2 \;<\; 3\; Y_{D\alpha}^2\; (M_{Q\alpha\alpha}^2 + M_{D\alpha\alpha}^2 + m_1^2)\;, \tag{11}$$

$$|T_{U\alpha\beta}|^2 \;<\; Y_{U\gamma}^2\; (M_{Q\alpha\alpha}^2 + M_{U\beta\beta}^2 + m_2^2)\;, \tag{12}$$

$$|T_{D\alpha\beta}|^2 \;<\; Y_{D\gamma}^2\; (M_{Q\alpha\alpha}^2 + M_{D\beta\beta}^2 + m_1^2)\;, \tag{13}$$

where $\alpha, \beta = 1, 2, 3,\ \alpha \neq \beta;\ \gamma = \mathrm{Max}(\alpha, \beta)$ and $m_1^2 = (m_{H^\pm}^2 + m_Z^2 \sin^2\theta_W)\sin^2\beta - \frac{1}{2}m_Z^2$, $m_2^2 = (m_{H^\pm}^2 + m_Z^2 \sin^2\theta_W)\cos^2\beta - \frac{1}{2}m_Z^2$. The Yukawa couplings of the up-type and down-type quarks are $Y_{U\alpha} = \sqrt{2}m_{u_\alpha}/v_2 = \frac{g}{\sqrt{2}}\frac{m_{u_\alpha}}{m_W \sin\beta}$ $(u_\alpha = u, c, t)$ and $Y_{D\alpha} = \sqrt{2}m_{d_\alpha}/v_1 = \frac{g}{\sqrt{2}}\frac{m_{d_\alpha}}{m_W \cos\beta}$ $(d_\alpha = d, s, b)$, with m_{u_α} and m_{d_α} being the running quark masses at the weak scale and g being the SU(2) gauge coupling. All soft-SUSY-breaking parameters are also assumed to be given at the weak scale. As SM parameters we take $m_W = 80.4$ GeV, $m_Z = 91.2$ GeV and the on-shell top-quark mass $m_t = 173.3$ GeV [29]. We have found that our results shown in the following are fairly insensitive to the precise value of m_t.

In addition to the constraints in Table 1 we impose the following limits:

1. The limit on $(m_{A^0}, \tan\beta)$ from the negative search for neutral MSSM Higgs bosons decaying into a tau pair (i.e. $A^0/H^0/h^0 \to \tau^+\tau^-$) at LHC [30] with m_{A^0} being the mass of the CP-odd neutral Higgs boson A^0.

2. The experimental limit on SUSY contributions on the electroweak ρ parameter [31]: $\Delta\rho\ (\mathrm{SUSY}) < 0.0012$.

3. The LEP limits on the SUSY particle masses [32]: $m_{\tilde{\chi}_1^\pm} > 103$ GeV, $m_{\tilde{\chi}_1^0} > 50$ GeV, where $m_{\tilde{\chi}_1^\pm}$ and $m_{\tilde{\chi}_1^0}$ are the masses of the lighter chargino and the lightest neutralino, respectively.

We take into account all the constraints listed in this section in all plots presented in this article. The constraints on the QFV parameters from $B(b \to s\gamma), \Delta M_{B_s}$ and the vacuum stability conditions are especially important for this study. For the computation of the observables (i.e. physical masses, decay branching ratios, ΔM_{B_s} and $\Delta\rho$(SUSY)) we use the public code SPheno v3.0 [33, 34] .

3 QFV three-body decays of gluino

If all squarks are heavier than the gluino and squark generation mixing occurs only between the second and third generation, one has the following QFV three-particle decays

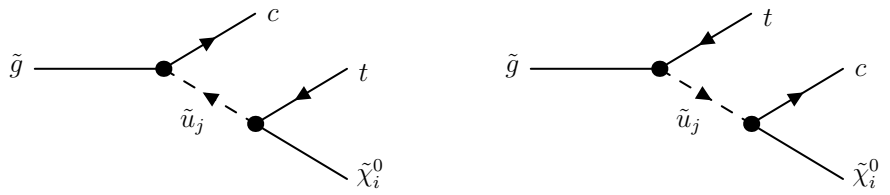

Figure 1: Feynman diagrams for $\tilde{g} \to c\,\bar{t}\,\tilde{\chi}_i^0$.

Table 2: Weak scale parameters at $Q = 1$ TeV for our prototype QFV scenario, except for m_{A^0} which is the pole mass (i.e. physical mass) of A^0. All of $T_{U\alpha\alpha}$ and $T_{D\alpha\alpha}$ are 0.

M_1	M_2	M_3	μ	$\tan\beta$	m_{A^0}
139 GeV	264 GeV	800 GeV	1000 GeV	10	800 GeV

	$\alpha = \beta = 1$	$\alpha = \beta = 2$	$\alpha = \beta = 3$
$M^2_{Q\alpha\beta}$	$(3150)^2$ GeV^2	$(3100)^2$ GeV^2	$(3050)^2$ GeV^2
$M^2_{U\alpha\beta}$	$(3000)^2$ GeV^2	$(2200)^2$ GeV^2	$(2150)^2$ GeV^2
$M^2_{D\alpha\beta}$	$(3000)^2$ GeV^2	$(2990)^2$ GeV^2	$(2980)^2$ GeV^2

of gluino into quarks and neutralinos $\tilde{\chi}_i^0$, $i = 1, 2, 3, 4$,

$$\tilde{g} \to c\,\bar{t}\,\tilde{\chi}_i^0,\ \bar{c}\,t\,\tilde{\chi}_i^0\,, \tag{14}$$

$$\tilde{g} \to s\,\bar{b}\,\tilde{\chi}_i^0,\ \bar{s}\,b\,\tilde{\chi}_i^0\,. \tag{15}$$

Table 3: Physical masses of the particles in the scenario of Table 2. m_{H^0} is the mass of the heavier CP-even neutral Higgs boson H^0.

$m_{\tilde{\chi}_1^0}$	$m_{\tilde{\chi}_2^0}$	$m_{\tilde{\chi}_3^0}$	$m_{\tilde{\chi}_4^0}$	$m_{\tilde{\chi}_1^+}$	$m_{\tilde{\chi}_2^+}$
139 GeV	281.3 GeV	1017.9 GeV	1021.7 GeV	281.5 GeV	1022.7 GeV

$m_{\tilde{g}}$	m_{h^0}	m_{H^0}	m_{A^0}	m_{H^+}
975 GeV	121.1 GeV	800.3 GeV	800 GeV	804 GeV

We will mainly focus on the decays into $\tilde{\chi}_1^0$. The corresponding Feynman diagrams for the decay $\tilde{g} \to c\bar{t}\tilde{\chi}_i^0$ are shown in Fig. 1. We have interference between the t and the u channel exchanges, as well as between the different $\tilde{u}_j$ exchange diagrams. In particular, there can be a strong destructive interference between the $\tilde{u}_l$ and $\tilde{u}_k$ contributions, if they

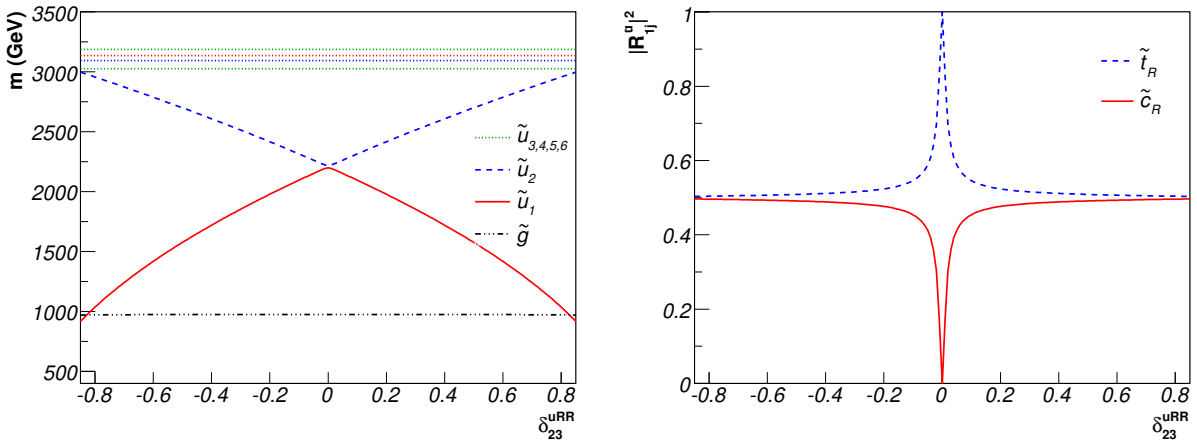

(a) (b)

Figure 2: (a) Up-type squark and gluino masses and (b) flavour decomposition of $\tilde{u}_1$ (i.e. $|R^{\tilde{u}}_{15}|^2 \equiv |\tilde{c}_R \text{ component}|^2$(full red line) and $|R^{\tilde{u}}_{16}|^2 \equiv |\tilde{t}_R \text{ component}|^2$ (dashed blue line)) as functions of the QFV parameter δ_{23}^{uRR}, with the other QFV parameters being zero, for the scenario of Table 2.

are mainly $\tilde{c}$ and $\tilde{t}$ mixtures and their masses are similar. For instance, if $\tilde{u}_l \sim \cos\theta \tilde{t}_R + \sin\theta \tilde{c}_R$ and $\tilde{u}_k \sim -\sin\theta \tilde{t}_R + \cos\theta \tilde{c}_R$ then the $\tilde{u}_l$ exchange contribution is $\sim \frac{(+\cos\theta \sin\theta)}{(p^2 - m^2_{\tilde{u}_l})}$ whereas the $\tilde{u}_k$ exchange contribution is $\sim \frac{(-\cos\theta \sin\theta)}{(p^2 - m^2_{\tilde{u}_k})}$. These two contributions almost cancel with each other for $m_{\tilde{u}_l} \approx m_{\tilde{u}_k}$. The suppression of this cancellation requires a large mass-splitting between the two squarks which can be induced by a large $\tilde{c}_R - \tilde{t}_R$ mixing term $M^2_{U_{23}}$ (or δ_{23}^{uRR}) even in case the $\tilde{c}_R$ mass parameter $M^2_{U_{22}}$ is similar to the $\tilde{t}_R$ mass parameter $M^2_{U_{33}}$. Moreover, in this case one has a very strong $\tilde{c}_R - \tilde{t}_R$ mixing. Therefore one can expect sizable QFV decay branching ratios for a large mass-splitting and hence for large values of δ_{23}^{uRR}. For the decays into down-type quarks one has analogous Feynman diagrams with the replacements $c \to s$, $t \to b$, $\tilde{u}_j \to \tilde{d}_j$.

There are also gluino three-body decays into charginos, such as $\tilde{g} \to c\bar{b}\tilde{}_1^-$, $s\bar{t}\tilde{\chi}_1^+$, etc.. We will, however, not discuss them explicitly here, although they are included in our branching ratio calculations.

We calculate the three-particle decay branching ratios of the gluino according to the diagrams in Fig. 1 and their charge conjugated ones, including the QFV couplings given in [6]. As basic SUSY parameters at the weak scale we take $M_1, M_2, M_3, \mu, \tan\beta, m_{A^0}, M^2_{Q\alpha\beta}$, $M^2_{U\alpha\beta}, M^2_{D\alpha\beta}, T_{U\alpha\beta}$ and $T_{D\alpha\beta}$, which we assume to be real. Here $M_{1,2,3}$ are the U(1), SU(2) and SU(3) gaugino mass parameters, respectively, and m_{A^0} is the pole mass (i.e. physical mass) of the Higgs boson A^0. We study in detail the QFV scenario based on the parameters of Table 2, given at the scale $Q = 1$ TeV, according to the SPA convention [35] except for m_{A^0} being the pole mass of A^0. The scenario of Table 2 satisfies all the constraints listed in Section 2; e.g. for the low energy observables we obtain

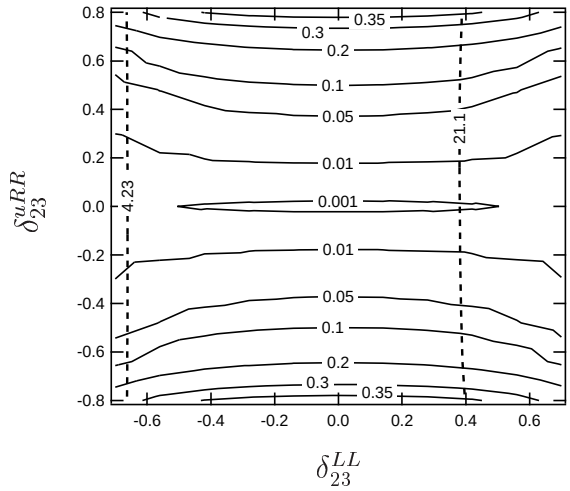

Figure 3: Contours of the QFV decay branching ratio $\mathrm{B}(\tilde{g} \to ct\tilde{\chi}_1^0)$ in the δ_{23}^{LL} - δ_{23}^{uRR} plane with the other QFV parameters being zero, for the scenario of Table 2 (solid lines). Also shown are the contours of $\Delta M_{B_s} = 21.1$ ps^{-1} and $10^4 \times \mathrm{B}(b \to s\gamma) = 4.23$ (dashed lines). The region between the two dashed lines is allowed by all the constraints mentioned in Section 2, including those from ΔM_{B_s} and $\mathrm{B}(b \to s\gamma)$.

$\Delta M_{B_s} = 19.01$ ps^{-1}, $\mathrm{B}(b \to s\gamma) = 3.46 \times 10^{-4}$, $\mathrm{B}(b \to s\, l^+ l^-) = 1.59 \times 10^{-6}$, $\mathrm{B}(b \to s\, \mu^+ \mu^-) = 5.02 \times 10^{-9}$, $R_{B\to\tau\nu}^{SUSY} = 0.99$, $m_{h^0} = 121.1$ GeV, $\Delta\rho$ (SUSY) $= 5.70 \times 10^{-5}$. We add to the parameters of Table 2 the QFV parameters $\delta_{23}^{LL}, \delta_{23}^{uRR}, \delta_{23}^{uRL}, \delta_{23}^{uLR}$ as well as $\delta_{23}^{dRR}, \delta_{23}^{dRL}, \delta_{23}^{dLR}$ (given also at $Q = 1$ TeV), and vary them in a range allowed by the constraints listed in Section 2. The physical masses for the case with all the QFV parameters being zero are shown in Table 3. They are calculated from the basic MSSM parameters at the one-loop level, taking into account the complete flavour structure [33]. We have found that these masses are fairly insensitive to the QFV parameters.

Note that in our case QFV left-right mixing effects, i.e. those due to $\delta_{23}^{uRL}, \delta_{23}^{uLR}$, $\delta_{23}^{dRL}, \delta_{23}^{dLR}$ cannot be significant. We show this for the left-right mixing parameter δ_{23}^{uRL}. Due to the vacuum stability condition (12) we have $|T_{U32}|^2 \lesssim Y_{U3}^2(M_{Q33}^2 + M_{U22}^2 + m_2^2) \approx M_{Q33}^2 + M_{U22}^2 \approx \mathrm{O}(10\ \mathrm{TeV}^2)$, because $Y_{U3} \approx 1$ and $m_2^2 \ll M_{Q33}^2 + M_{U22}^2$. Therefore, $|\delta_{23}^{uRL}| = \frac{v_2}{\sqrt{2}} \frac{|T_{U32}|}{\sqrt{M_{Q33}^2 M_{U22}^2}} \lesssim \frac{v_2}{\sqrt{2}} \sqrt{\frac{M_{Q33}^2 + M_{U22}^2}{M_{Q33}^2 M_{U22}^2}} \approx 0.1$. Analogously, the parameters $\delta_{23}^{uLR}, \delta_{23}^{dRL}, \delta_{23}^{dLR}$ are also constrained to be very small due to the vacuum stability conditions. Therefore, the most relevant QFV parameters in our study are $\delta_{23}^{LL}, \delta_{23}^{uRR}, \delta_{23}^{dRR}$.

Fig. 2a shows the physical masses of the up-type squarks $\tilde{u}_1, ..., \tilde{u}_6$ as functions of the QFV parameter δ_{23}^{uRR}, with all the other QFV parameters being zero, for the scenario of Table 2. All the constraints mentioned in Section 2 are fulfilled in the shown range. Masses of all the down-type squarks $\tilde{d}_i$ are about 3 TeV in this range. For $|\delta_{23}^{uRR}| \lesssim 0.8$ all squarks are heavier than the gluino. In Fig. 2b we show the flavour decomposition of $\tilde{u}_1$. For $|\delta_{23}^{uRR}| \gtrsim 0.2$, $\tilde{u}_1$ is practically a full mixture of $\tilde{c}_R$ and $\tilde{t}_R$. For $|\delta_{23}^{uRR}| \lesssim 0.88$ the flavour decomposition of $\tilde{u}_2$ is similar to that of $\tilde{u}_1$ with $\tilde{c}_R$ and $\tilde{t}_R$ interchanged.

In Fig. 3 we show contours of the branching ratio $\mathrm{B}(\tilde{g} \to ct\tilde{\chi}_1^0) \equiv \mathrm{B}(\tilde{g} \to c\bar{t}\tilde{\chi}_1^0) + \mathrm{B}(\tilde{g} \to \bar{c}t\tilde{\chi}_1^0)$ in the $\delta_{23}^{LL} - \delta_{23}^{uRR}$ plane together with contours of $10^4 \times \mathrm{B}(b \to s\gamma) = 4.23$ and $\Delta M_{B_s} = 21.1\ \mathrm{ps}^{-1}$, where the other parameters are fixed as in Table 2. The branching ratio $\mathrm{B}(\tilde{g} \to ct\tilde{\chi}_1^0)$ can reach values larger than 35%. As can be seen, in the range $-0.65 \lesssim \delta_{23}^{LL} \lesssim 0.35$, the $\mathrm{B}(b \to s\gamma)$ and the ΔM_{B_s} constraints are fulfilled. In Ref. [36] it is shown that also the ρ-parameter data may constrain the flavour off-diagonal elements of the squark mass matrices, in particular the $\delta_{\alpha\beta}^{LL}$ entries. However, in our case the ρ-parameter practically does not give constraints for two reasons. First, we have negligible left-right squark mixing implying that the left-squark sector is almost decoupled from the right-squark sector. Second, the mass matrices of the left up-type squarks and the left down-type squarks are related by the $SU(2)_L$ symmetry leading to approximately the same masses and mixing matrices for the up-type and down-type squarks.

In Fig. 4 the branching ratios $\mathrm{B}(\tilde{g} \to ct\tilde{\chi}_1^0)$, $\mathrm{B}(\tilde{g} \to c\bar{c}\tilde{\chi}_1^0)$ and $\mathrm{B}(\tilde{g} \to t\bar{t}\tilde{\chi}_1^0)$ are shown as functions of δ_{23}^{uRR}, with the other QFV parameters being zero and the other parameters fixed as in Table 2. All the constraints mention in Section 2 are fulfilled in the shown range. One can see that the QFV decay branching ratio $\mathrm{B}(\tilde{g} \to ct\tilde{\chi}_1^0)$ can reach 40% and that in the range $0.6 \lesssim |\delta_{23}^{uRR}| \lesssim 0.8$ the QFV decay branching ratio $\mathrm{B}(\tilde{g} \to ct\tilde{\chi}_1^0)$ is even larger than the quark-flavour conserving (QFC) branching ratio $\mathrm{B}(\tilde{g} \to t\bar{t}\tilde{\chi}_1^0)$. For $|\delta_{23}^{uRR}| \gtrsim 0.8$, the two-body decays into $\tilde{u}_1$ dominate because $\tilde{u}_1$ becomes lighter than the gluino (see Fig. 2a). The reason for this large QFV decay branching ratio is as follows: For $0.6 \lesssim |\delta_{23}^{uRR}| \lesssim 0.8$, all squarks other than $\tilde{u}_1$ (including down-type squarks) are very heavy (see Fig. 2(a)), which leads to the dominance of the $\tilde{u}_1$ exchange contribution in the gluino decays. In this δ_{23}^{uRR} range the $\tilde{u}_1,\ \tilde{u}_2$ are strong mixtures of $\tilde{c}_R$ and $\tilde{t}_R$ and the mass-splitting between $\tilde{u}_1$ and $\tilde{u}_2$ is very large, preventing a strong destructive interference between the $\tilde{u}_1$ and $\tilde{u}_2$ exchange contributions in this δ_{23}^{uRR} range (see Fig. 2). This gives the large QFV decay branching ratio $\mathrm{B}(\tilde{g} \to ct\tilde{\chi}_1^0)$. Note that $\tilde{u}_1 (\sim \tilde{c}_R + \tilde{t}_R)$ couples to $\tilde{\chi}_1^0 (\approx \tilde{B}^0)$ and practically does not couple to $\tilde{\chi}_2^0 (\approx \tilde{W}^0)$ and $\tilde{\chi}_1^\pm (\approx \tilde{W}^\pm)$ (see Table 2). Moreover, $\tilde{\chi}_{3,4}^0$ and $\tilde{\chi}_2^\pm$ are very heavy in the QFV scenario considered here (see Table 3.). $\tilde{B}^0$ and $\tilde{W}^{0,\pm}$ are the U(1) and SU(2) gauginos (the bino and winos), respectively.

On the other hand, as can be seen in Fig. 3, the dependence of $\mathrm{B}(\tilde{g} \to ct\tilde{\chi}_1^0)$ on the $\tilde{c}_L$ - $\tilde{t}_L$ mixing parameter δ_{23}^{LL} is much weaker than that on δ_{23}^{uRR}. This is mainly due to the fact that in our scenario the left-squarks $(\tilde{c}_L, \tilde{t}_L)$ are significantly heavier than the right-squarks $(\tilde{c}_R, \tilde{t}_R)$ and that the left-squark coupling to $\tilde{\chi}_1^0$ ($\sim$ bino) is small. Hence, the contributions of the left-squark exchanges to $B(\tilde{g} \to ct\tilde{\chi}_1^0)$ are suppressed, leading to the very small effect of the $\tilde{c}_L - \tilde{t}_L$ mixing parameter δ_{23}^{LL} on the QFV decay branching ratio. As a consequence, for $|\delta_{23}^{uRR}| \lesssim 0.4$ the QFV decay branching ratio $\mathrm{B}(\tilde{g} \to ct\tilde{\chi}_1^0)$ is smaller than 5% even for larger allowed values of $|\delta_{23}^{LL}|$.

The gluino can also have QFV decays into down-type quarks with sizeable branching ratios if the δ_{23}^{dRR} or δ_{23}^{LL} are unequal to zero. As an example, in Fig. 5 we show a contour plot of the QFV decay branching ratio $\mathrm{B}(\tilde{g} \to sb\tilde{\chi}_1^0) \equiv \mathrm{B}(\tilde{g} \to s\bar{b}\tilde{\chi}_1^0) + \mathrm{B}(\tilde{g} \to \bar{s}b\tilde{\chi}_1^0)$ in the δ_{23}^{dRR} - δ_{23}^{LL} plane for the scenario of Table 2. The dashed contour lines for $\Delta M_{B_s} = 14.5\ \mathrm{ps}^{-1}$ and $21.1\ \mathrm{ps}^{-1}$ show the region $-0.38 \lesssim \delta_{23}^{LL} \lesssim 0.12$ allowed by all the constraints mentioned in Section 2, including the $\mathrm{B}(b \to s\gamma)$ constraint. Note that in this case the

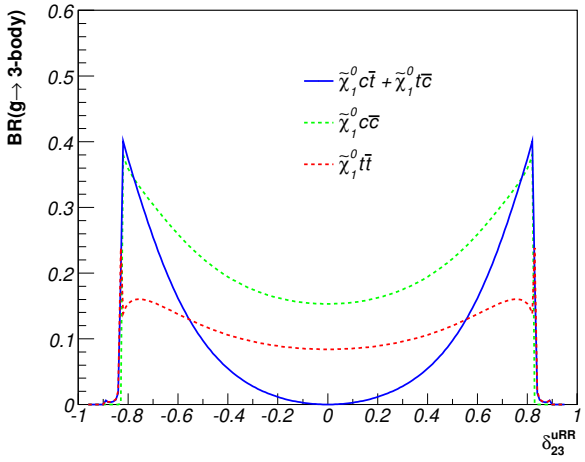

Figure 4: The branching ratios of the decays $\tilde{g} \to c\bar{t}\tilde{\chi}_1^0 + \bar{c}t\tilde{\chi}_1^0$, $\tilde{g} \to c\bar{c}\tilde{\chi}_1^0$ and $\tilde{g} \to t\bar{t}\tilde{\chi}_1^0$ as functions of δ_{23}^{uRR} for the other QFV parameters being zero and the other parameters are fixed as in Table 2.

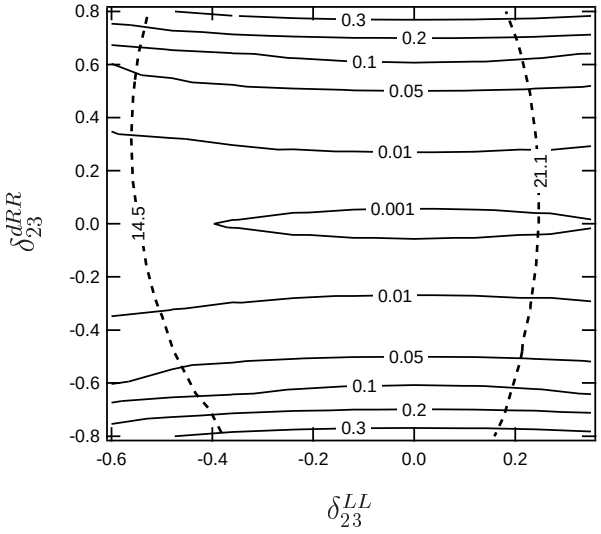

Figure 5: Contours of the QFV decay branching ratio $\mathrm{B}(\tilde{g} \to sb\tilde{\chi}_1^0)$ in the δ_{23}^{LL} - δ_{23}^{dRR} plane, with the other QFV parameters being zero for the scenario of Table 2, but with the values of $M_{U\alpha\alpha}^2$ and $M_{D\alpha\alpha}^2$ interchanged (solid lines). Also shown are the contour lines for $\Delta M_{B_s} = 14.5$ ps^{-1} and $\Delta M_{B_s} = 21.1$ ps^{-1} (dashed lines). The region between the two dashed lines is allowed by all the constraints mentioned in Section 2, including the ΔM_{B_s} constraint.

ΔM_{B_s} constraint is significantly stronger than the $\mathrm{B}(b \to s\gamma)$ constraint in the whole $\delta_{23}^{LL} - \delta_{23}^{dRR}$ plane. $\mathrm{B}(\tilde{g} \to sb\tilde{\chi}_1^0)$ can reach values larger than 30%. The reason for this sizable QFV decay branching ratio is similar to that for the large QFV decay branching

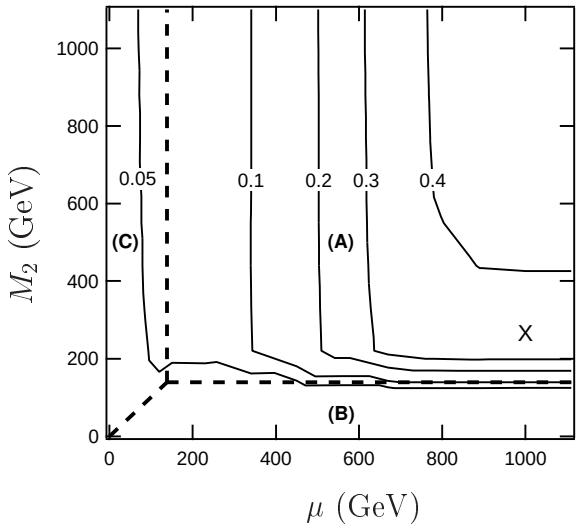

Figure 6: Contour plot for $B(\tilde{g} \to ct\tilde{\chi}_1^0)$ (solid lines) in the $\mu - M_2$ plane for $\delta_{23}^{uRR} = 0.8$, the other QFV parameters being zero, and the other parameters specified as in Table 2 with $M_1 = 139$ GeV. Region (A): bino-like LSP region; region (B): wino-like LSP region; region (C): higgsino-like LSP region. The point "X" corresponds to our reference scenario given in Table 2: $M_2 = 264$ GeV, $\mu = 1000$ GeV.

ratio B$(\tilde{g} \to ct\tilde{\chi}_1^0)$. The dependence of this QFV decay branching ratio on δ_{23}^{LL} is again much weaker than that on δ_{23}^{dRR}.

We also would like to note that we have found a scenario giving QFV three-body decay branching ratios B$(\tilde{g} \to ct\tilde{\chi}_1^0)$ (or B$(\tilde{g} \to sb\tilde{\chi}_1^0)$) of about 50% for a gluino mass of ~ 1 TeV, still satisfying all the relevant constraints. In such a scenario, however, the heavier squarks have masses of about 6 TeV, while the lightest squark heavier than the gluino has a mass of about 1 TeV.

4 Influence of the neutralino/chargino parameters on the QFV three-body gluino decays

As the squark generation mixing enters into the squark-quark-neutralino/chargino couplings, here we study how the pattern of the QFV gluino decays depends on the parameters of the neutralino-chargino sector. First we show in Fig. 6 a contour plot of the branching ratio $B(\tilde{g} \to ct\tilde{\chi}_1^0)$ in the $\mu - M_2$ plane for $\delta_{23}^{uRR} = 0.8$, the other QFV parameters being zero, and the other parameters fixed as in Table 2. In the whole plane $m_{\tilde{g}} \approx 972$ GeV. As one can see, this branching ratio is larger than 10% for $\mu \gtrsim 350$ GeV. We indicate the regions where the LSP is bino-, wino-, or higgsino-like. The largest QFV decay branching ratio $B(\tilde{g} \to ct\tilde{\chi}_1^0)$ is in the bino-like LSP region reaching up to $\sim 40\%$.

In the following we discuss the dependence of the QFV decay branching ratios of the

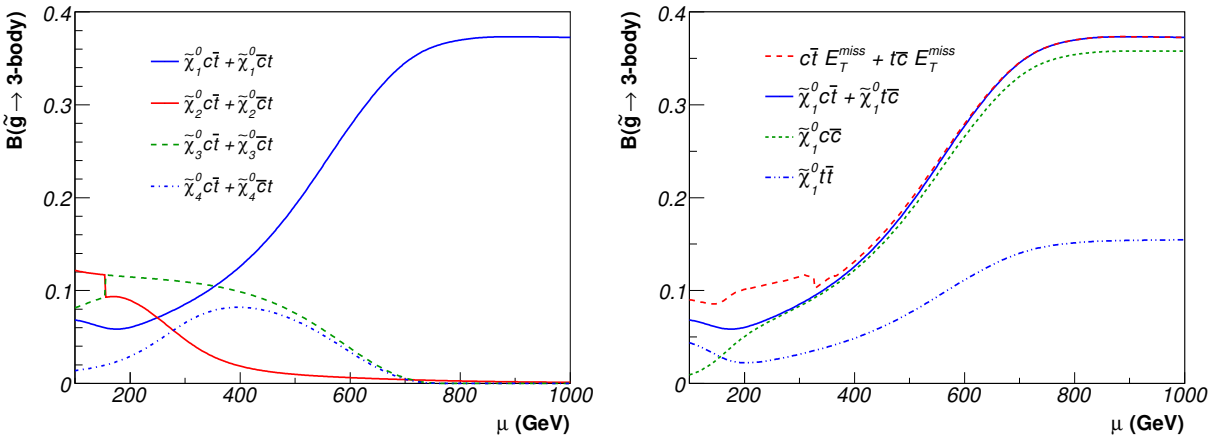

(a) (b)

Figure 7: The μ dependence of the QFV and QFC gluino decay branching ratios for $\delta_{23}^{uRR} = 0.8$, the other QFV parameters being zero, for the scenario given in Table 2. (a) Branching ratios of the decays $\tilde{g} \to c\bar{t}\tilde{\chi}_i^0 + \bar{c}t\tilde{\chi}_i^0$, $i = 1, ..., 4$ as a function of μ. (b) Branching ratios of the decays $\tilde{g} \to c\bar{c}\tilde{\chi}_1^0$, $\tilde{g} \to t\bar{t}\tilde{\chi}_1^0$, $\tilde{g} \to c\bar{t}\tilde{\chi}_1^0 + \bar{c}t\tilde{\chi}_1^0$ and $\tilde{g} \to c\bar{t}E_{\rm T}^{mis} + \bar{c}tE_{\rm T}^{mis}$ as a function of μ.

gluino on the higgsino mass parameter μ in more detail. In Fig. 7 we show this dependence for $\delta_{23}^{uRR} = 0.8$, the other QFV parameters being zero, and the other parameters fixed as in Table 2. In the whole range $m_{\tilde{g}} \approx 972$ GeV and the constraints mentioned in Section 2 are satisfied. The branching ratios of the QFV gluino decays $\tilde{g} \to c\bar{t}\tilde{\chi}_i^0 + \bar{c}t\tilde{\chi}_i^0$, $i = 1, ..., 4$ are shown in Fig. 7a. For $\mu \gtrsim M_1$ the bino component of $\tilde{\chi}_1^0$ is increasing and hence the branching ratio of $\tilde{g} \to c\bar{t}(\bar{c}t)\tilde{\chi}_1^0$ increases. For $\mu \gtrsim 700$ GeV this branching ratio is about 36%, being roughly a factor of 2 larger than that for $\tilde{g} \to t\bar{t}\tilde{\chi}_1^0$. For $|\mu| \lesssim M_1$, $\tilde{\chi}_1^0$ and $\tilde{\chi}_2^0$ are essentially higgsinos, and the branching ratio of $\tilde{g} \to c\bar{t}(\bar{c}t)\tilde{\chi}_1^0$ is less than 10%. The reason is that the QFV decays into the higher neutralinos and the charginos become more important. Note that $|\mu| \lesssim 100$ GeV is excluded by the LEP limit on the $m_{\tilde{\chi}_1^\pm}$. Furthermore, the final state $c\bar{t}E_{\rm T}^{mis} + \bar{c}tE_{\rm T}^{mis}$ can contain contributions from the higher neutralino modes $c\bar{t}(\bar{c}t)\tilde{\chi}_i^0$, $i \geq 2$, with the invisible decays of $\tilde{\chi}_i^0 \to \tilde{\chi}_1^0\nu\bar{\nu}$, where $E_{\rm T}^{mis}$ is missing transverse energy. Therefore, we show in Fig. 7b a plot where these contributions are included (dashed red line). One can clearly see that for $\mu \lesssim 320$ GeV the contributions of the invisible decays of the higher neutralinos (see Fig. 7a) are important. For comparison in Fig. 7b the QFC branching ratios $\mathrm{B}(\tilde{g} \to c\bar{c}\tilde{\chi}_1^0)$ and $\mathrm{B}(\tilde{g} \to t\bar{t}\tilde{\chi}_1^0)$ are also shown.

The situation is quite different if $M_1 > M_2$. In this case, for $\mu \gtrsim M_2$ the $\tilde{\chi}_1^0$ is essentially a wino which does not couple to $\tilde{c}_R$ and $\tilde{t}_R$ leading to a small branching ratio of $\tilde{g} \to c\bar{t}(\bar{c}t)\tilde{\chi}_1^0$. On the other hand, a large branching ratio of $\tilde{g} \to c\bar{t}(\bar{c}t)\tilde{\chi}_2^0$ can be expected, because for $|\mu| \gtrsim M_1$, $\tilde{\chi}_2^0$ becomes bino-like.

Next we discuss the dependence of the QFV gluino decay branching ratios on the

SU(2) gaugino mass parameter M_2. In Fig. 8 we show this dependence fixing $M_1 = 264$ GeV, $\mu = 600$ GeV, $\delta_{23}^{uRR} = 0.8$, the other QFV parameters being zero, and the other parameters fixed as in Table 2. In the shown range $m_{\tilde{g}} \approx 972$ GeV and all the constraints mentioned in Section 2 are satisfied. As just explained above, in Fig. 8a, for $M_2 \lesssim M_1$ the branching ratio of the decay $\tilde{g} \to c\bar{t}(\bar{c}t)\tilde{\chi}_1^0$ is almost zero, while that for $\tilde{g} \to c\bar{t}(\bar{c}t)\tilde{\chi}_2^0$ is large ($\approx 24\%$). For $M_2 \gtrsim M_1$ the roles of $\tilde{\chi}_1^0$ and $\tilde{\chi}_2^0$ are interchanged and therefore the decay $\tilde{g} \to c\bar{t}(\bar{c}t)\tilde{\chi}_1^0$ becomes dominant with a branching ratio of about 25%. Note that the range $M_2 \lesssim 100$ GeV is excluded by the LEP chargino mass limit mentioned in Section 2: $m_{\tilde{\chi}_1^\pm} > 103$ GeV. At $M_2 \approx \mu$ there is again a level crossing. The $\tilde{\chi}_4^0$ is higgsino-like for $M_2 \lesssim \mu$ and becomes wino-like for $M_2 \gtrsim \mu$.

In Fig. 8b the branching ratios for the decays $\tilde{g} \to c\bar{b}(\bar{c}b)\tilde{\chi}_k^\pm$ as a function of M_2 are shown. The level crossing of $\tilde{\chi}_1^\pm$ and $\tilde{\chi}_2^\pm$ at $M_2 \approx \mu$ is clearly seen.

In the following we discuss in more detail a typical scenario with a higgsino-like LSP ($\mu < M_1, M_2$) and one with a wino-like LSP ($M_2 < M_1, \mu$). As an example for the higgsino-like LSP scenario, we choose the parameters as given in Table 4(a), with the squark mass parameters as in Table 2. We fix the QFV parameter $\delta_{23}^{uRR} = 0.8$ and the other QFV parameters equal zero. In this scenario all experimental and theoretical constraints mentioned in Section 2 are fulfilled. The relevant masses for the neutralinos and the charginos are given in Table 4(b). We show the most important QFV decay branching ratios in Table 4(c). In this scenario $\tilde{\chi}_{1,2}^0$ and $\tilde{\chi}_1^\pm$ are almost higgsinos and hence their couplings to $\tilde{u}_1 (\sim \tilde{c}_R + \tilde{t}_R)$ are significantly enhanced by the large top-quark Yukawa coupling, which results in the sizable branching ratios of the QFV decays into $\tilde{\chi}_{1,2}^0$ and $\tilde{\chi}_1^\pm$. Since $\mathrm{B}(\tilde{\chi}_2^0 \to \tilde{\chi}_1^0 \nu\bar{\nu})$ is relatively large ($= 18.4\%$), the sum of the branching ratios for the $\tilde{g}$ decays into the final states $(c\bar{t} + E_{\mathrm{T}}^{mis})$ and $(\bar{c}t + E_{\mathrm{T}}^{mis})$ is sizable ($= 9.0\%$). The leptonic $\tilde{\chi}_1^\pm$ decays $\tilde{\chi}_1^\pm \to \mu^\pm \nu_\mu \tilde{\chi}_1^0$ and $\tilde{\chi}_1^\pm \to e^\pm \nu_e \tilde{\chi}_1^0$ have a branching ratio of approximately 11.2% each, because W exchange dominates. Therefore, from the gluino decays into $\tilde{\chi}_1^\pm$ one gets final states $b\bar{c}(\bar{b}c) + \mu^\pm(e^\pm) + E_{\mathrm{T}}^{mis}$ with a branching ratio of 5.0%. This has to be compared with the expectation from MFV which is of the order of 10^{-4}, as it is proportional to $|V_{cb}|^2$.

Next we discuss a scenario where the LSP is wino-like, with the parameters as given in Table 5(a), the squark mass parameters as in Table 2, $\delta_{23}^{uRR} = 0.8$ and the other QFV parameters being zero. Again, all the constraints are satisfied. The masses of the neutralinos and charginos are given in Table 5(b). The relevant QFV gluino decay branching ratios are shown in Table 5(c). As in this case $\mathrm{B}(\tilde{\chi}_2^0 \to \tilde{\chi}_1^0 \nu\bar{\nu}) = 4.1\%$, the sum of the branchung ratios for the final states $(c\bar{t} + E_{\mathrm{T}}^{mis})$ and $(\bar{c}t + E_{\mathrm{T}}^{mis})$ is 6%. As $\mathrm{B}(\tilde{\chi}_1^+ \to \mu^+ \nu_\mu \tilde{\chi}_1^0) = \mathrm{B}(\tilde{\chi}_1^+ \to e^+ \nu_e \tilde{\chi}_1^0) = 13.2\%$, one has $\mathrm{B}(\tilde{g} \to b\bar{c}\mu^+ \nu_\mu \tilde{\chi}_1^0) = \mathrm{B}(\tilde{g} \to \bar{b}c\mu^- \bar{\nu}_\mu \tilde{\chi}_1^0) = \mathrm{B}(\tilde{g} \to b\bar{c}e^+ \nu_e \tilde{\chi}_1^0) = \mathrm{B}(\tilde{g} \to \bar{b}ce^- \bar{\nu}_e \tilde{\chi}_1^0) = 0.8\%$. Hence, the signature $b\bar{c}$ (or $\bar{b}c$) plus a lepton ($\mu^\pm$ or $e^\pm$) plus E_{T}^{mis} has a probability of about 3%.

Summarizing the discussion of this section we can say that the branching ratios of the QFV three-particle gluino decays depend not only on the generation mixing in the squark sector, but also quite strongly on the parameters of the neutralino/chargino sector.

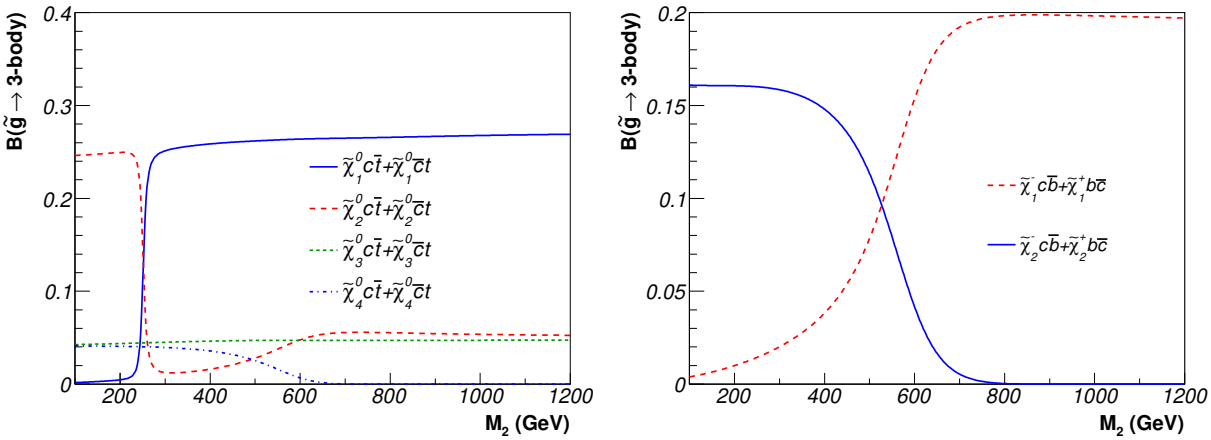

(a) (b)

Figure 8: The M_2 dependence of the QFV gluino decay branching ratios for $M_1 = 264$ GeV, $\mu = 600$ GeV, $\delta_{23}^{uRR} = 0.8$, the other QFV parameters being zero, and the other parameters fixed as in Table 2. (a) Branching ratios of the decays $\tilde{g} \to c\bar{t}\tilde{\chi}_i^0 + \bar{c}t\tilde{\chi}_i^0$, $i = 1, ..., 4$ as a function of M_2. (b) Branching ratios of the decays $\tilde{g} \to c\bar{b}\tilde{\chi}_k^- + \bar{c}b\tilde{\chi}_k^+$, $k = 1, 2$ as a function of M_2.

Table 4: Weak scale parameters at $Q = 1$ TeV (except for m_{A^0} being the pole mass), the corresponding neutralino and chargino masses and some important branching ratios for a scenario with a higgsino-like LSP, where $m_{\tilde{g}} = 972$ GeV.

(a) Weak scale parameters at $Q = 1$ TeV.

M_1	M_2	M_3	μ	$\tan\beta$	m_{A^0}
139 GeV	264 GeV	800 GeV	120 GeV	10	800 GeV

(b) Neutralino and chargino masses.

$m_{\tilde{\chi}_1^0}$	$m_{\tilde{\chi}_2^0}$	$m_{\tilde{\chi}_3^0}$	$m_{\tilde{\chi}_4^0}$	$m_{\tilde{\chi}_1^+}$	$m_{\tilde{\chi}_2^+}$
87.0 GeV	133.1 GeV	158.3 GeV	310.1 GeV	109.3 GeV	310.1 GeV

(c) Important branching ratios.

B($\tilde{g} \to c\bar{t}\tilde{\chi}_1^0$)	B($\tilde{g} \to c\bar{t}\tilde{\chi}_2^0$)	B($\tilde{g} \to b\bar{c}\tilde{\chi}_1^+$)	B($\tilde{\chi}_2^0 \to \tilde{\chi}_1^0\nu\bar{\nu}$)	B($\tilde{\chi}_1^+ \to \mu^+\nu_\mu\tilde{\chi}_1^0$)
3.4 %	6.1 %	11.2 %	18.4 %	11.2 %

Table 5: Weak scale parameters at $Q = 1$ TeV (except for m_{A^0} being the pole mass), the corresponding neutralino and chargino masses and some important branching ratios for a scenario with a wino-like LSP, where $m_{\tilde{g}} = 972$ GeV.

(a) Weak scale parameters at $Q = 1$ TeV.

M_1	M_2	M_3	μ	$\tan\beta$	m_{A^0}
400 GeV	300 GeV	800 GeV	350 GeV	10	800 GeV

(b) Neutralino and chargino masses.

$m_{\tilde{\chi}_1^0}$	$m_{\tilde{\chi}_2^0}$	$m_{\tilde{\chi}_3^0}$	$m_{\tilde{\chi}_4^0}$	$m_{\tilde{\chi}_1^+}$	$m_{\tilde{\chi}_2^+}$
275.5 GeV	362.6 GeV	376.4 GeV	433.1 GeV	280.0 GeV	407.1 GeV

(c) Important branching ratios.

$\mathrm{B}(\tilde{g} \to c\bar{t}\tilde{\chi}_1^0)$	$\mathrm{B}(\tilde{g} \to c\bar{t}\tilde{\chi}_2^0)$	$\mathrm{B}(\tilde{g} \to b\bar{c}\tilde{\chi}_1^+)$	$\mathrm{B}(\tilde{\chi}_2^0 \to \tilde{\chi}_1^0\nu\bar{\nu})$	$\mathrm{B}(\tilde{\chi}_1^+ \to \mu^+\nu_\mu\tilde{\chi}_1^0)$
2.5 %	6.3 %	5.8 %	4.1 %	13.2 %

5 Measurability of the QFV gluino three-body decays

We calculate the relevant gluino production cross sections at leading order using the WHIZARD/O'MEGA packages [37, 38] where we have implemented the model described in Section 2 with squark generation mixing in its most general form. We use the CTEQ6L global parton density fit [39] for the parton distribution functions and take $Q = m_{\tilde{p}_1} + m_{\tilde{p}_2}$ for the factorization scale, where $\tilde{p}_1$ and $\tilde{p}_2$ are the sparticle pair produced. The QCD coupling $\alpha_s(Q)$ is also evaluated (at the two-loop level) at this scale Q. Due to the heavy squarks in our reference scenario of Table 2, the dominant gluino production process at LHC is $pp \to \tilde{g}\tilde{g}X$, where X contains beam-jets only. For the scenario of Table 2 the corresponding cross section is practically independent of δ_{23}^{uRR} and is about 170 fb (3 fb) at $\sqrt{s} = 14$ TeV (7 TeV). (Note that $m_{\tilde{g}} = 975$ GeV and 972 GeV for $\delta_{23}^{uRR} = 0$ and 0.8, respectively.) The sum of the cross sections of the other gluino production processes, such as $pp \to \tilde{g}\tilde{q}_1X,\ \tilde{g}\tilde{q}_2X,\ \tilde{g}\tilde{\chi}_1^0X,\ \tilde{g}\tilde{\chi}_2^0X$, is two orders of magnitude smaller than that of $pp \to \tilde{g}\tilde{g}X$.

In Fig. 9 we show the signal rates due to $pp \to \tilde{g}\tilde{g}X$, with X containing beam-jets only, at $\sqrt{s} = 14$ TeV, where at least one of the pair-produced gluinos decays as $\tilde{g} \to c\bar{t}(\bar{c}t)\tilde{\chi}_1^0$, as a function of δ_{23}^{uRR} for the scenario of Table 2. All the constraints mentioned in Section 2 are satisfied in the range $|\delta_{23}^{uRR}| \lesssim 0.85$. The rate of the final state $cc\bar{t}\bar{t}E_{\mathrm{T}}^{mis}X$, produced in the case when both gluinos decay like $\tilde{g} \to c\bar{t}\tilde{\chi}_1^0$, reaches 7 fb for $|\delta_{23}^{uRR}| = 0.8$ (full blue line), yielding 700 events for an integrated luminosity of 100 fb^{-1}. The charge conjugated final state $\bar{c}\bar{c}ttE_{\mathrm{T}}^{mis}X$ has the same rate. The full red line shows the rate for the QFV case where one gluino decays as $\tilde{g} \to c\bar{t}\tilde{\chi}_1^0$ and the other one as $\tilde{g} \to \bar{c}t\tilde{\chi}_1^0$ plus the QFC case with one $\tilde{g} \to c\bar{c}\tilde{\chi}_1^0$ and the other $\tilde{g} \to t\bar{t}\tilde{\chi}_1^0$. The dashed red line presents the rate for the QFC case only. One can see that the QFV signal has a rate of about 14 fb for $|\delta_{23}^{uRR}| = 0.8$. The green lines show the case of one gluino decaying as $\tilde{g} \to c\bar{t}\tilde{\chi}_1^0$, and the

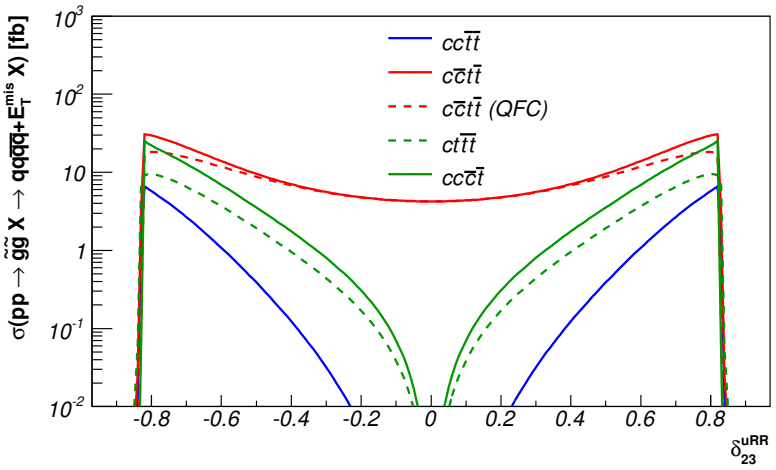

Figure 9: Signal rates for $pp \to \tilde{g}\tilde{g}X$ at $\sqrt{s} = 14$ TeV where at least one of the gluinos decays as $\tilde{g} \to c\bar{t}(\bar{c}t)\tilde{\chi}_1^0$, as a function of δ_{23}^{uRR} with the other QFV parameters being zero and the other parameters fixed as in Table 2. Shown are the rates for the final states with $cc\bar{t}\bar{t}E_{\rm T}^{mis}$ (full blue line), $c\bar{c}t\bar{t}E_{\rm T}^{mis}$ (QFV + QFC) (full red line), $c\bar{c}t\bar{t}E_{\rm T}^{mis}$ (QFC only) (dashed red line), $ct\bar{t}\bar{t}E_{\rm T}^{mis}$ (dashed green line), $cc\bar{c}\bar{t}E_{\rm T}^{mis}$ (full green line).

other one as $\tilde{g} \to c\bar{c}\tilde{\chi}_1^0$ (full green line) or $\tilde{g} \to t\bar{t}\tilde{\chi}_1^0$ (dashed green line). These rates reach 25 fb and 10 fb, respectively, for $|\delta_{23}^{uRR}| = 0.8$. The charge conjugated final states have the same rates.

A characteristic feature of a three-particle decay of the gluino is the invariant mass distribution of the two produced quarks. We calculate the invariant mass distributions $\mathrm{d}\Gamma(\tilde{g} \to u_j\bar{u}_k\tilde{\chi}_1^0)/(\Gamma_{tot}(\tilde{g})\ dM_{u_j\bar{u}_k})$, where $M_{u_j\bar{u}_k}$ is the invariant mass of the two-quark system $u_j\bar{u}_k$, $M_{u_j\bar{u}_k}^2 = (p_{u_j} + p_{\bar{u}_k})^2$. In Fig. 10 we show these distributions for $\tilde{g} \to t\bar{t}\tilde{\chi}_1^0, c\bar{c}\tilde{\chi}_1^0, c\bar{t}\tilde{\chi}_1^0 + \bar{c}t\tilde{\chi}_1^0$ with $\delta_{23}^{uRR} = 0.8$ and the other QFV parameters being zero for the scenario of Table 2. In contrast to the case where the squarks are lighter than the gluino and the gluino decays via real squarks [11], no edge structure appears. However, the thresholds and the shapes of the distributions are very different. The endpoint is at $(m_{\tilde{g}} - m_{\tilde{\chi}_1^0})$. The thresholds are at $2m_c, m_c + m_t$ and $2m_t$, respectively. Measuring these distributions could be helpful for separating the QFV decays into $c\bar{t}\tilde{\chi}_1^0 + \bar{c}t\tilde{\chi}_1^0$ from the QFC decays.

A typical $\tilde{g}\tilde{g}$ production event has at least four large-p_T jets and large $E_{\rm T}^{mis}$. An event with a QFV gluino decay $\tilde{g} \to c\bar{t}\tilde{\chi}_1^0(\bar{c}t\tilde{\chi}_1^0)$ should contain at least one top (anti-top) quark in the final state, which must be identified. This is possible by using the decay $t \to bW^{\pm}$ with the $W^{\pm}$ decaying into two jets. For this purpose a special method was proposed in [40]. Charm tagging would be extremely helpful for a clear identification of the QFV gluino decay $\tilde{g} \to \bar{c}t\tilde{\chi}_1^0(c\bar{t}\tilde{\chi}_1^0)$. If this is not possible one could search for the decay $\tilde{g} \to \bar{q}t\tilde{\chi}_1^0(q\bar{t}\tilde{\chi}_1^0), q \neq t$. Typical signatures of QFV $\tilde{g}$ pair events are: $t(\text{or } \bar{t}) + 3$ jets $+ E_{\rm T}^{mis} + X$,

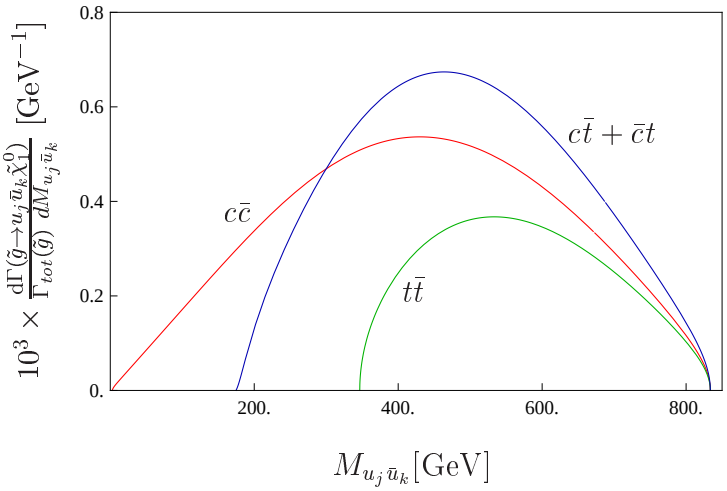

Figure 10: Invariant mass distributions of two up-type quarks from the decay $\tilde{g} \to u_j \bar{u}_k \tilde{\chi}_1^0$, with $\delta_{23}^{uRR} = 0.8$, the other QFV parameters being zero, and the other parameters fixed as in Table 2.

$t + t$ (or $\bar{t} + \bar{t}$) + 2 jets + $E_{\rm T}^{mis} + X$ and $t + t + \bar{t}$ (or $\bar{t} + \bar{t} + t$) + 1 jet + $E_{\rm T}^{mis} + X$, where X contains beam-jets only. Note, that the signal events $t + t$ (or $\bar{t} + \bar{t}$) + 2jets + $E_{\rm T}^{mis} + X$ can practically not be produced in the MSSM (nor in the SM) with QFC.

The rate of a possible SUSY background from pair production of squarks, such as $pp \to \tilde{q}\bar{\tilde{q}}X$ with $\tilde{q} \to c\tilde{\chi}_1^0$, $\bar{\tilde{q}} \to \bar{t}\tilde{\chi}_1^0$ is much smaller than that of the signal of gluino pair production due to the larger squark masses. As shown in the SUSY searches by ATLAS and CMS [12, 13], the SM backgrounds, such as QCD multijets, $W^{\pm}$ + jets, Z^0 + jets, $t\bar{t}$ and single top production, can be strongly reduced by appropriate selection cuts.

6 Conclusions

We have studied QFV decays of gluino within the MSSM in the case that all squarks are heavier than the gluino and, hence, the gluino has only three-particle decays. Starting from the most general squark mass matrix, we have assumed mixing between the second and the third squark generations in the up and down sectors. We have taken into account all relevant experimental constraints from SUSY particles and Higgs searches as well as from precision data in the B meson sector. Furthermore we have respected the vacuum stability conditions for the trilinear coupling matrices. It has turned out that of all QFV parameters the parameters δ_{23}^{uRR}, δ_{23}^{dRR} and δ_{23}^{LL} play the most important role in our study. We have concentrated on the QFV decays $\tilde{g} \to c\bar{t}(\bar{c}t)\tilde{\chi}_1^0$ and $\tilde{g} \to b\bar{s}(\bar{b}s)\tilde{\chi}_1^0$ which presumably have the clearest signatures for the presence of QFV in the MSSM. We have studied these within a prototype scenario with gluino mass $m_{\tilde{g}} \approx 1$ TeV and squarks with masses between ~ 1 TeV and ~ 3 TeV, where the lightest squarks are $\tilde{c}_R - \tilde{t}_R$ mixtures (or $\tilde{s}_R - \tilde{b}_R$ mixtures). These QFV decay branching ratios can reach up to 40% (35%). We

have paid special attention to the dependence of the QFV decay branching ratios on the chargino/neutralino parameters. In this context we have considered three cases where the lightest neutralino is bino-, wino- and higgsino-like, respectively. We have found that the QFV decay branching ratios depend strongly also on the chargino/neutralino parameters.

As in our scenario the squarks are heavier than the gluino, the dominant gluino production process at LHC is gluino pair production, $pp \to \tilde{g}\tilde{g}X$. We have calculated the rates for the various signatures stemming from QFV gluino decays as well as the invariant mass distributions of the two-quark system $c\bar{t}+\bar{c}t, c\bar{c}, t\bar{t}$ in the final states. We have found that the rates of the resulting QFV signatures, like $pp \to tc\bar{c}\bar{c}E_{\rm T}^{mis}X$ and $pp \to tt\bar{c}\bar{c}E_{\rm T}^{mis}X$, are significant at LHC. This could have an important influence on the search for gluinos and the determination of the basic MSSM parameters at LHC.

Acknowledgments

This work is supported by the "Fonds zur Förderung der wissenschaftlichen Forschung (FWF)" of Austria, project No. I 297-N16, and by the DFG, project No. PO-1337/2-1. B. H. acknowledges support by the Landes-Exzellenzinitiative Hamburg.

References

[1] C. Amsler *et al.* [Particle Data Group], Phys. Lett. B **667** (2008) 1.

[2] T. Plehn, M. Rauch, M. Spannowsky, Phys. Rev. D **80** (2009) 114027 [arXiv:0906.1803, hep-ph].

[3] A. J. Buras, P. Gambino, M. Gorbahn, S. Jager and L. Silvestrini, Phys. Lett. B **500** (2001) 161 [arXiv:hep-ph/0007085].

[4] G. D'Ambrosio, G. F. Giudice, G. Isidori and A. Strumia, Nucl. Phys. B **645** (2002) 155 [arXiv:hep-ph/0207036].

[5] A. L. Kagan, G. Perez, T. Volansky and J. Zupan, Phys. Rev. D **80** (2009) 076002 [arXiv:0903.1794, hep-ph].

[6] G. Bozzi, B. Fuks, B. Herrmann, M. Klasen, Nucl. Phys. B **787** (2007) 1-54 [arXiv: 0704.1826, hep-ph].

[7] B. Fuks, B. Herrmann, M. Klasen, Nucl. Phys .B **810** (2009) 266-299 [arXiv:0808.1104, hep-ph].

[8] A. Bartl, H. Eberl, B. Herrmann, K. Hidaka, W. Majerotto, W. Porod, Phys. Lett. B **698** (2011) 380-388 [arXiv:1007.2100, hep-ph].

[9] M. Bruhnke, B. Herrmann, W. Porod, JHEP **09:006** (2010) 1-35 [arXiv:1007.5483, hep-ph].

[10] T. Hurth and W. Porod, JHEP **0908** (2009) 087 [arXiv:0904.4574, hep-ph].

[11] A. Bartl, K. Hidaka, K. Hohenwarter-Sodek, T. Kernreiter, W. Majerotto, W. Porod, Phys. Lett. B **679** (2009) 260-266 [arXiv:0905.0132, hep-ph].

[12] G. Aad et al., ATLAS Collaboration, Phys. Rev. Lett. **106** (2011) 131802 [arXiv:1102.2357[hep-ex]]; G. Aad et al., ATLAS Collaboration, Phys. Lett. B **701** (2011) 186 [arXiv:1102.5290[hep-ex]]; G. Aad et al., ATLAS Collaboration, Phys. Lett. B **701** (2011) 398 [arXiv:1103.4344[hep-ex]]; G. Aad et al., ATLAS Collaboration, Eur. Phys. J. C **71** (2011) 1 [arXiv:1103.6214[hep-ex]]; S. Caron [ATLAS collaboration], Prepared for the 46th Rencontres de Moriond on Electroweak Interactions and Unified Theories, La Thuile, Italy, 13 - 20 Mar 2011 [arXiv:1106.1009[hep-ex]].

[13] V. Khachatryan et al., CMS Collaboration, Phys. Lett. B **698** (2011) 196 [arXiv:1101.1628[hep-ex]]; S. Chatrchyan et al., CMS Collaboration, arXiv:1103.1348[hep-ex], Submitted to JHEP; S. Chatrchyan et al., CMS Collaboration, arXiv:1106.4503[hep-ex], Accepted by JHEP; S. Chatrchyan et al., CMS Collaboration, arXiv:1107.1279[hep-ex], Submitted to Phys. Rev. D; S. Chatrchyan et al., CMS Collaboration, JHEP **07** (2011) 113 [arXiv:1106.3272[hep-ex]].

[14] W. Ehrenfeld, plenary talk at "19th International Conference on Supersymmetry and Unification of Fundamental Interactions (SUSY2011)", Fermilab, Batavia, 28 Aug - 2 Sep 2011.

[15] I. Melzer-Pellmann, plenary talk at "19th International Conference on Supersymmetry and Unification of Fundamental Interactions (SUSY2011)", Fermilab, Batavia, 28 Aug - 2 Sep 2011; S. Chatrchyan et al., CMS Collaboration, arXiv:1109.2352[hep-ex].

[16] M. Flowerdew, parallel talk at "19th International Conference on Supersymmetry and Unification of Fundamental Interactions (SUSY2011)", Fermilab, Batavia, 28 Aug - 2 Sep 2011.

[17] B. C. Allanach et al., Comput. Phys. Commun. **180** (2009) 8 [arXiv:0801.0045, hep-ph].

[18] F. Gabbiani, E. Gabrielli, A. Masiero and L. Silvestrini, Nucl. Phys. B **477** (1996) 321 [arXiv:hep-ph/9604387].

[19] W. S. Hou, Phys. Rev. **D48** (1993) 2342.

[20] M. Carena, A. Menon, R. Noriega-Papaqui, A. Szynkman, C. E. M. Wagner, Phys. Rev. **D74** (2006) 015009 [arXiv:hep-ph/0603106]; see also P. Ball, R. Fleischer, Eur. Phys. J. **C48** (2006) 413-426 [arXiv:hep-ph/0604249].

[21] K. Trabelsi, plenary talk at ICHEP2010, PoS (ICHEP 2010) 566.

[22] M. Misiak *et al.*, Phys. Rev. Lett. **98** (2007) 022002 [arXiv:hep-ph/0609232]; see also T. Hurth, E. Lunghi and W. Porod, Nucl. Phys. B **704** (2005) 56 [arXiv:hep-ph/0312260].

[23] M. Iwasaki *et al.* [Belle Collaboration], Phys. Rev. **D72** (2005) 092005 [arXiv:hep-ex/0503044]; B. Aubert *et al.* [BABAR Collaboration], Phys. Rev. Lett. **93** (2004) 081802 [arXiv:hep-ex/0404006].

[24] T. Huber, T. Hurth and E. Lunghi, Nucl. Phys. B **802** (2008) 40 [arXiv:0712.3009, hep-ph].

[25] G. Borissov, plenary talk at ICHEP2010, PoS (ICHEP 2010) 531.

[26] S. Schael *et al.* [ALEPH Collaboration, DELPHI Collaboration, L3 Collaboration, OPAL Collaboration and LEP Working Group for Higgs Boson Searches], Eur. Phys. J. **C47** (2006) 547-587 [arXiv:hep-ex/0602042].

[27] B. C. Allanach, A. Djouadi, J. L. Kneur, W. Porod and P. Slavich, JHEP **0409** (2004) 044 [arXiv:hep-ph/0406166].

[28] J. A. Casas and S. Dimopoulos, Phys. Lett. B **387** (1996) 107 [arXiv:hep-ph/9606237].

[29] E. Shabalina, plenary talk at ICHEP2010, PoS (ICHEP 2010) 561.

[30] M. L. Vazquez Acosta, plenary talk at "19th International Conference on Supersymmetry and Unification of Fundamental Interactions (SUSY2011)", Fermilab, Batavia, 28 Aug - 2 Sep 2011; S. Chatrchyan et al., CMS Collaboration, Phys. Rev. Lett.106 (2011) 231801 [arXiv:1104.1619[hep-ex]]; G. Aad et al., ATLAS Collaboration, arXiv:1107.5003[hep-ex], Submitted to Phys. Lett. B.

[31] G. Altarelli, R. Barbieri, F. Caravaglios, Int. J. Mod. Phys. **A13** (1998) 1031-1058 [arXiv:hep-ph/9712368].

[32] G. Sguazzoni, Proceedings of 'ICHEP02 - 31st International Conference on High Energy Physics', 24-31 July 2002, Amsterdam, The Nederlands, Eds. S. Bentvelson, P. de Jong, J. Koch, E. Laenen, p. 709, [arXiv:hep-ex/0210022]; P. Lutz, the same proceedings, p. 735.

[33] W. Porod, Comput. Phys. Commun. **153** (2003) 275 [arXiv:hep-ph/0301101]; The code SPheno v3.0 can be obtained from:
http://www.physik.uni-wuerzburg.de/∼porod/SPheno.html

[34] W. Porod and F. Staub, [arXiv:1104.1573, hep-ph].

[35] J. A. Aguilar-Saavedra et al., Eur. Phys. J. **C46** (2006) 43-60 [arXiv:hep-ph/0511344].

[36] S. Heinemeyer, W. Hollik, F. Merz and S. Penaranda, Eur. Phys. J. C **37** (2004) 481 [arXiv:hep-ph/0403228].

[37] W. Kilian, T. Ohl and J. Reuter, [arXiv:0708.4233, hep-ph].

[38] M. Moretti, T. Ohl and J. Reuter, [arXiv:hep-ph/0102195].

[39] J. Pumplin et al., JHEP **0207** (2002) 012, [arXiv:hep-ph/0201195].

[40] J. Hisano, K. Kawagoe, R. Kitano, M. M. Nojiri, Phys. Rev. D **66** (2002) 115004 [arXiv:hep-ph/0204078]; J. Hisano, K. Kawagoe, M. M. Nojiri, Phys. Rev. D **68** (2003) 035007 [arXiv:hep-ph/0304214].